ANNUAL PROGRESS REPORT

1998 - 1999

INVESTIGATION OF A NEW CLASS OF LOW-PROFILE MULTI-LAYER PRINTED ANTENNAS

PRINCIPAL INVESTIGATOR:
AHMAD HOORFAR, Ph.D.

DEPARTMENT OF ELECTRICAL AND
COMPUTER ENGINEERING
VILLANOVA UNIVERSITY
VILLANOVA, PA 19085

PREPARED FOR:

OFFICE OF NAVAL RESEARCH
ARLINGTON, VA 22217

OCTOBER, 1999

INVESTIGATION OF A NEW CLASS OF LOW-PROFILE MULTI-LAYER PRINTED ANTENNAS

Period: 10/98 - 9/99

Principal Investigator: Ahmad Hoorfar

Research Associate: Changhua Wan

Graduate Student: Yuan Liu

ABSTRACT

This progress report outlines our research efforts on modeling, analyses and optimization of multi-layered printed antennas for high gain applications. Our research during this interim period has resulted in progress in the following four areas. 1) Performance analysis of a linear array of Yagi-like printed sub-array antennas. The effects of mutual couplings on gain and pattern degradation of previously optimized Yagi-like structures are investigated for various array configurations that one may encounter in a practical design. 2) Development of an electromagnetic optimization engine based on Method of Moments and Evolutionary Programming for design of multi-layer printed antennas. During this interim period, this code has been extended to include printed patch antennas of arbitrary shapes. In addition, the use of various mutation operators to speed-up the optimization process has been investigated in details where it has been found that a Cauchy mutation operator can significantly speed-up the optimal design of antenna structures particularly when the corresponding objective functions include many local optima. 3) Design of circularly polarized (CP) high gain multilayer antenna elements. The design feasibility of a high gain CP microstrip patch antenna is demonstrated for MSAT application where a gain of more than 11.6 dBi with an axial ratio of less than 1.1 dB is obtained. 4) Theoretical investigation of Gain Enhancement methods for the Yagi-like antennas printed in a multi-layer anisotropic medium. During this interim period, the conditions for obtaining high gain together with high radiation efficiency for a microstrip dipole antenna embedded in a multi-layer anisotropic medium have been derived. In particular, it's shown that by a proper selection of anisotropy ratios and thickness of the layers, it is possible to obtain two high gain beams at θ_E and θ_H in E and H planes respectively. In addition, the physics of these high gain fields are investigated in terms of the leaky-wave radiation.

TABLE OF CONTENTS

I. INTRODUCTION

This progress report summarizes our research efforts on modeling, analyses and optimization of multi-layered printed antennas for various applications in communications and radar that may require high gain, wide bandwidth, multi-band and/or circular polarization. The report covers the time-period, October 1998 – September 1999. The technical contributions made during this period include:

i) The radiation performance of Yagi-like stacked printed sub-array antennas when used as elements in an array environment have been analyzed. In particular, the effect of mutual coupling on gain and far-field pattern of previously optimized Yagi-like structures are investigated for various array configurations that one may encounter in practice. It's found that gain degradation due to the surface-waves and coupling effects can be substantial

ii) The electromagnetic optimization engine, which its development was reported in our last annual report [1], has now been extended to include multi-layer printed patch antennas of arbitrary shapes. This numerical engine is based on a hybrid combination of Method of Moments (MOM) and Evolutionary Programming (EP). In addition, the convergence rates of two different mutation operators, namely Gaussian and Cauchy, in the EP optimization process have been investigated in details. It has been found that the Cauchy mutation operator can significantly speed-up the global optimal design of antenna structures whose objective functions posses many local optima and when a few or no constraints are put on the design parameters. We have applied this optimization engine to optimize the gain of a stacked Yagi-like array of narrow strip dipoles as well as Yagi-like array of rectangular microstrip patch elements.

iii) In order to demonstrate the design feasibility of multi-layer high gain microstrip antennas with Circular polarization (CP), a three-layer rectangular patch antenna is designed for MSAT application. A MOM analysis of this structure shows a gain of more than 11.6 dBi with an axial ratio of less than 1.1 dB at an operating frequency of 1.6 GHz. In addition, the mutual coupling effects on gain and axial ratio of these antennas in an array environment has been analyzed.

iv) As a first step toward the extension of the Yagi-like concept to antennas printed in multi-layer anisotropic media, we have analyzed the conditions for obtaining high gain together with high radiation efficiency for a microstrip dipole antenna embedded in a multi-layer anisotropic medium. It's shown that by a proper selection of anisotrpy ratios and thickness of the layers, it is possible to obtain two high gain beams at θ_E and θ_H in E and H planes respectively. Examples of various 3 and 5 layer configurations have been studied. In addition, the physics of these high gain fields are investigated in terms of the leaky-wave radiation.

II. PERFORMANCE ANALYSIS OF A LINEAR ARRAY OF YAGI-LIKE PRINTED SUB-ARRAY ANTENNAS

In our last annual technical report [1] we presented the analysis of a microstrip Yagi-like antenna which consists of a reflector (ground-plane), a driver and a finite number of embedded director strip elements (Figure 1). This structure gives more degrees of freedom (i.e., the dielectric constants of the layers) when optimizing its design. It can also be made conformal to various shapes and surfaces. In addition, unlike the gain-enhancement techniques reported for an embedded microstrip antenna [2,3], without directors, the Yagi-like structures can achieve high gains without the need for very high permittivity dielectric layers. In fact we have previously shown that it is possible to optimize a three-layer structures with dielectric constant of ε_r =2 for a gain as high as 10 dBi or more. The Yagi gain enhancement technique, however, results in narrow gain and impedance bandwidths. The question, therefore, arises on how these Yagi-like structures perform when used as radiating elements in an array environment.

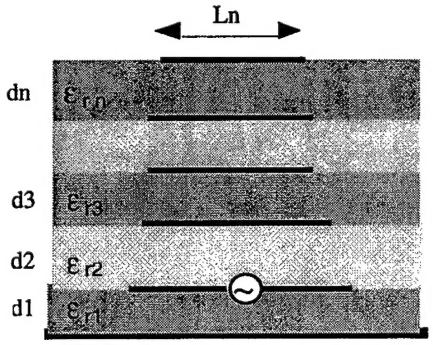

Figure 1: A Yagi stacked microstrip array in a multi-layered medium

Let us consider a 3 layer microstrip Yagi-like antenna with $\varepsilon_{r1} = \varepsilon_{r2} = \varepsilon_{r3}$ =2. Table I shows the design parameters for three optimized cases reported in the last annual report [1]. The width of each strip element is w = 0.02 λ_0, where λ_0 is the free-space wavelength. Case 1, which results in more than 13.5 dBi of gain, was optimized with a constraint on the input reactance, X_{in} =0 (i.e., resonant driver element) but with no constraint on the input resistance, R_{in}. Solution in Case 2, was obtained subject to an additional constraint of R_{in} >10 ohms, while in Case 3, in addition to the above constraints, a constraint was also put on the maximum total thickness: $D = d_1 + d_2 + d_3 < 0.5$ λ_d. Gains for these three cases as functions of normalized frequency are depicted in Figure 2, while the corresponding E-plane far-field patterns are shown in Figure 3.

We now examine the performance of these three cases when they are used to form a 2-element as well as a 5-element linear array. We have investigated both collinear as well as side-by-side element arrangements.

Table 1: Previously Optimized 3-layer 'Yagi-like' stacked microstrip array

	Gain (dBi)	d1 (λ_d)	d2 (λ_d)	d3 (λ_d)	xdri (λ_0)	xdri(1) (λ_0)	xdri(2) (λ_0)	Rin (Ω)	Rad. Eff. η_s
Case 1	13.57	0.240	0.120	0.360	0.3180	0.3295	0.3889	0.109	93 %
Case 2	11.10	0.299	0.252	0.491	0.2955	0.3005	0.3327	14.43	96 %
Case 3	9.88	0.125	0.092	0.230	0.2838	0.2881	0.3686	20.32	81 %

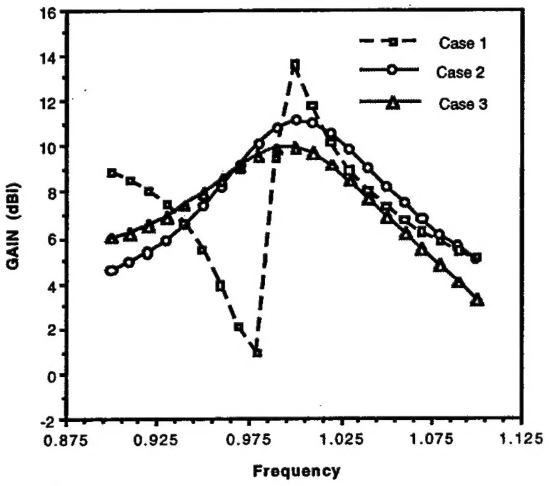

Figure 2: Gain versus frequency

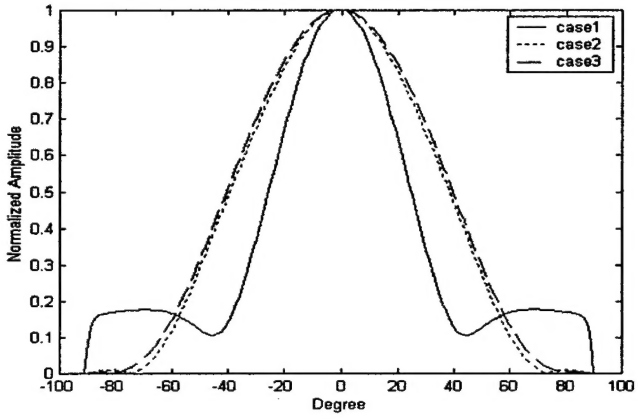

Figure 3: E-plane far-field patterns

A. Collinear Yagi-like Arrays

Figures 4 and 5 show a two and a five element collinear Yagi-like array with an inter-element spacing of $d_0 = 0.5\ \lambda_0$, respectively. The element axis and array axis is both assumed to be along the x-axis. Far-field patterns in the $\phi = 0$ plane are plotted when the radiating elements correspond to one of the three optimized cases in Table 1. In order to show the effect of mutual couplings, the far-fields computed when the couplings are neglected (i.e., element pattern multiply by array factor) are included for comparison. As can be seen the coupling has minimal effects on the pattern for the 2-element array except perhaps for Case 1 which as was shown in Figure 2 is very narrow band and therefore more susceptible to mutual coupling and surface-wave effects. The effects of mutual coupling are more pronounced for the 5-element array in Figure 5. The pattern is greatly influenced when the radiating elements are those of Case1 and the least affected by the coupling effects when the elements are those of Case 3 which has a relatively broad band frequency response. One can particularly notice the large increases in the side-lobe-levels. The pattern degradation for Case 1 is partly an indication that the surface-wave reduction mechanism, resulted from optimization of the lengths of the elements and the thickness of the dielectric layers, has been disturbed by the mutual coupling effects.

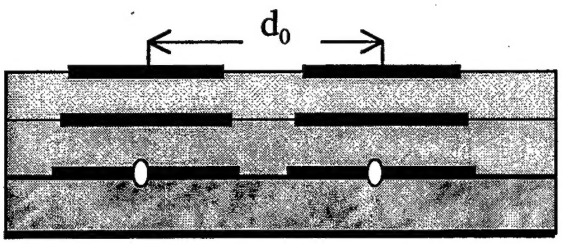

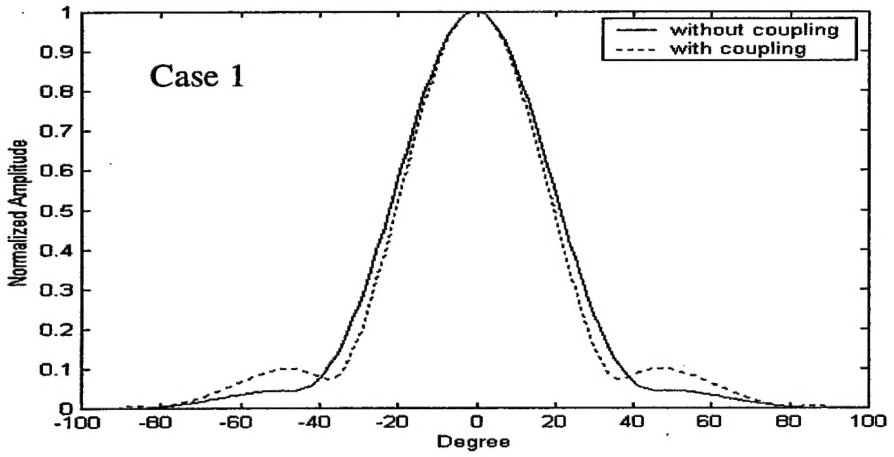

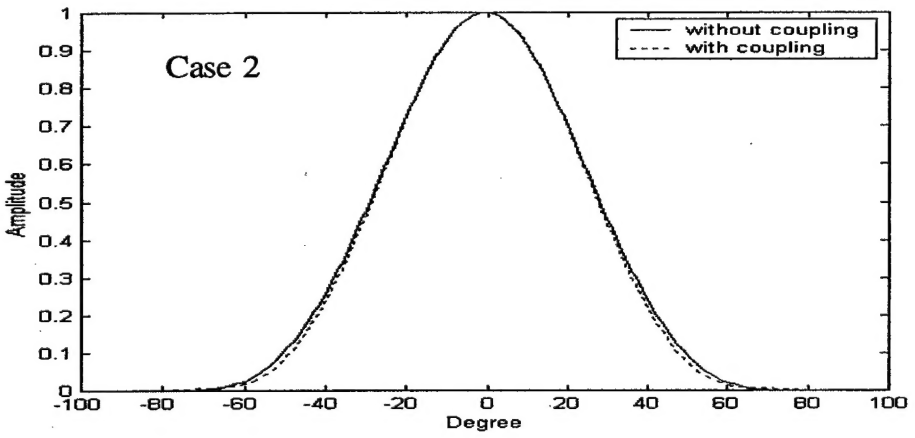

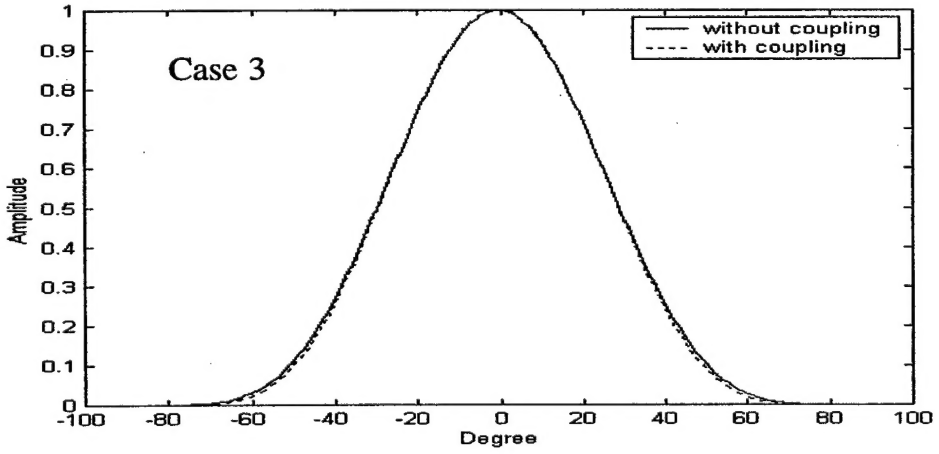

Figure 4: Patterns in the $\phi = 0$ plane for a 2-element collinear array of Yagi-like antennas

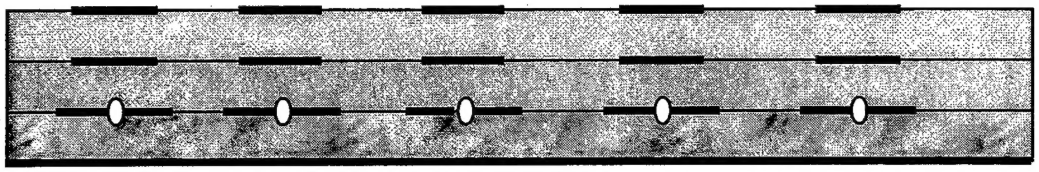

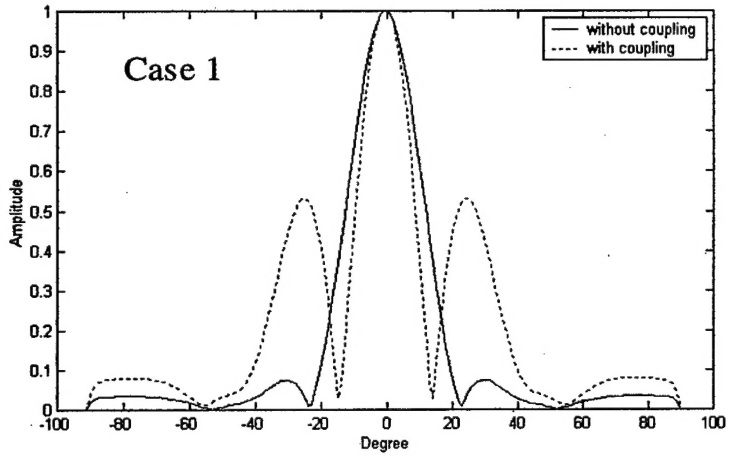

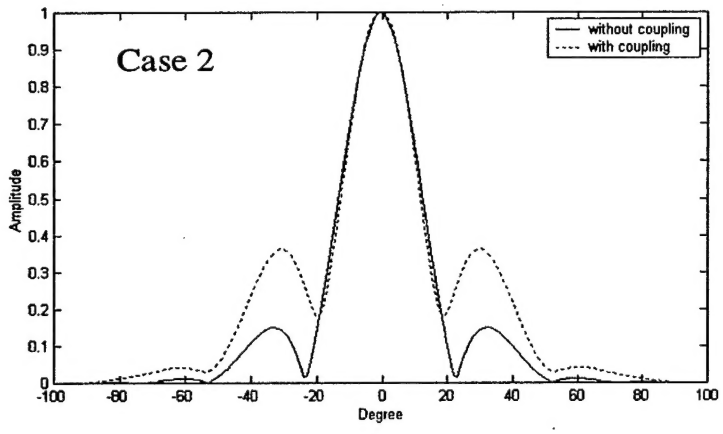

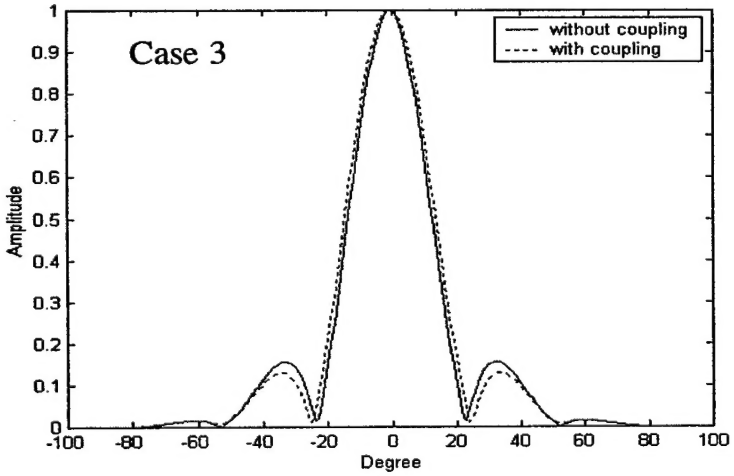

Figure 5: Patterns in the $\phi = 0$ plane for a 5-element collinear array of Yagi-like antennas

B. Side-by-side Yagi-like Arrays

Figures 6, 7 and 8 show the results for two and five element Yagi-like arrays when the radiating elements are positioned in a side-by-side arrangement. The element axis is x-axis and the array axis is assumed to be along the y-axis. For the five element array, patterns in both the $\phi = 0$ and the $\phi = 90°$ planes are plotted. Again, the effect of mutual coupling is more pronounced for Case 1 particularly in the $\phi = 0°$ plane where the pattern without the coupling effects is basically that of a single Yagi-like element shown in Figure 3. The patterns in the $\phi = 0$ plane for Case 2 and Case 3 are relatively unaffected by the coupling effects because of their broader radiating elements frequency responses.

Finally, gain and radiation efficiency (i.e., ratio of the radiated power to the total of the radiated plus the surface-wave powers) are tabulated in Tables 2 through 4 for the three Yagi-like element cases. Arraying does not significantly increase the gain for Case 1 because of the strong coupling effects. Without coupling effects one would expect an increase of approximately 3 and 7 dBi , over the gain of an isolated element, for a 2-element and a 5-element array, respectively. The results in these tables together with the above far-field patterns clearly show that in order to fully take advantage of the Yagi-like gain enhancement technique, one should globally optimize gain of the whole array, in the presence of the mutual coupling effects, rather than an element in isolation.

Table 2: Case 1

	Single element	2 elements collinear	2 elements side by side	5 elements collinear	5 elements side by side
Gain (dBi)	13.57	14.41	13.70	16.07	15.29
Efficiency	92.7%	96.5%	89.8%	94.6%	88.6%
Gain improvement over single element (dBi)		1.33	1.34	3.83	4.42

Table 3: Case 2

	Single element	2 elements collinear	2 elements side by side	5 elements collinear	5 elements side by side
Gain (dBi)	11.10	12.43	12.44	14.93	15.52
Efficiency	96.7%	97.3%	94.8%	97.3%	94.1%
Gain improvement over single element (dBi)	–	1.33	1.34	3.83	4.42

Table 4: Case 3

	Single element	2 elements collinear	2 elements side by side	5 elements collinear	5 elements side by side
Gain (dBi)	9.88	11.31	11.55	14.32	14.86
Efficiency	81%	77.1%	83.2%	76.9%	84.9%
Gain improvement over single element (dBi)	–	1.43	1.67	4.44	4.98

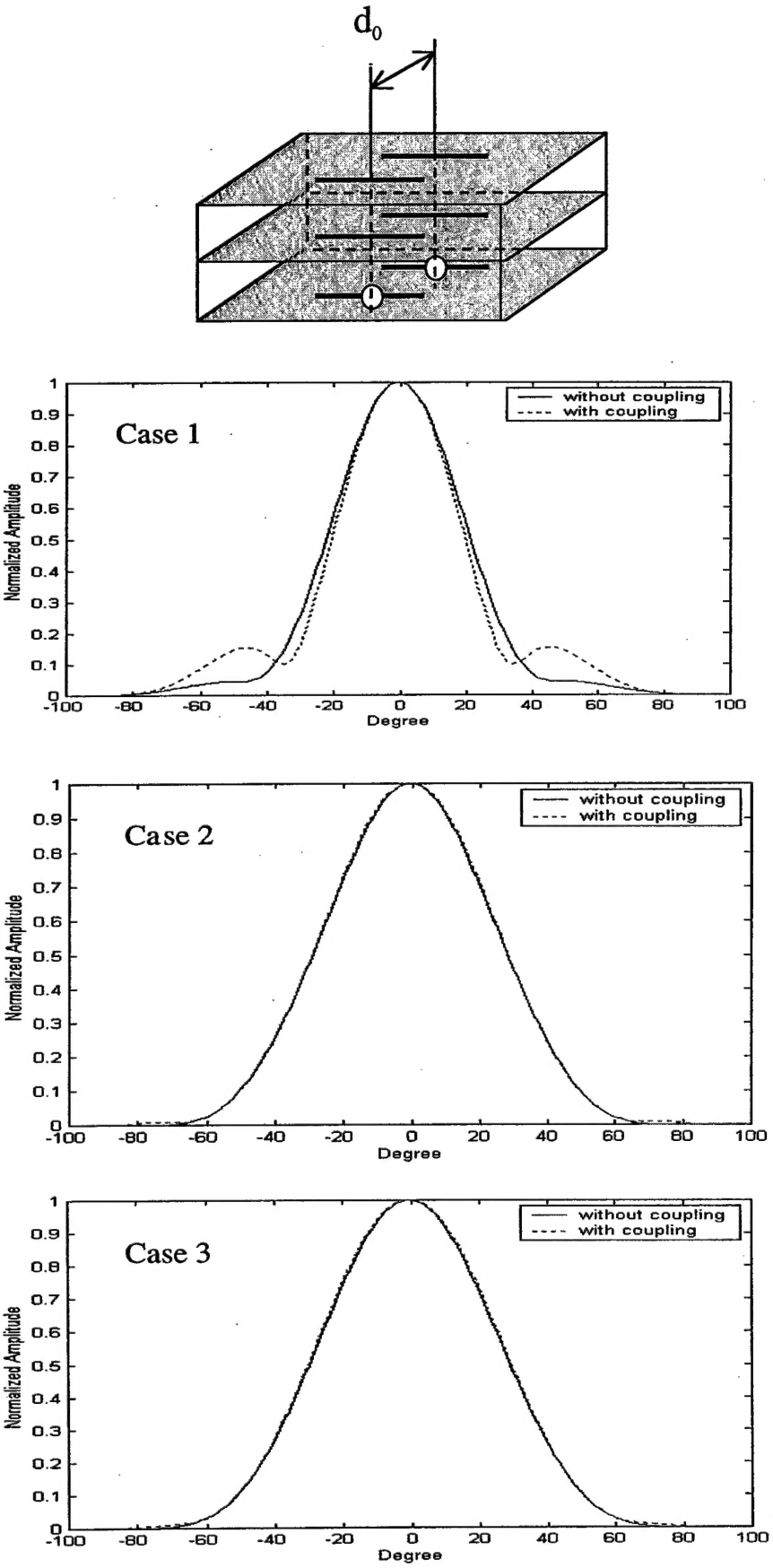

Figure 6: Patterns in the $\phi = 90°$ plane for a 2-element side-by-side array of Yagi-like antennas

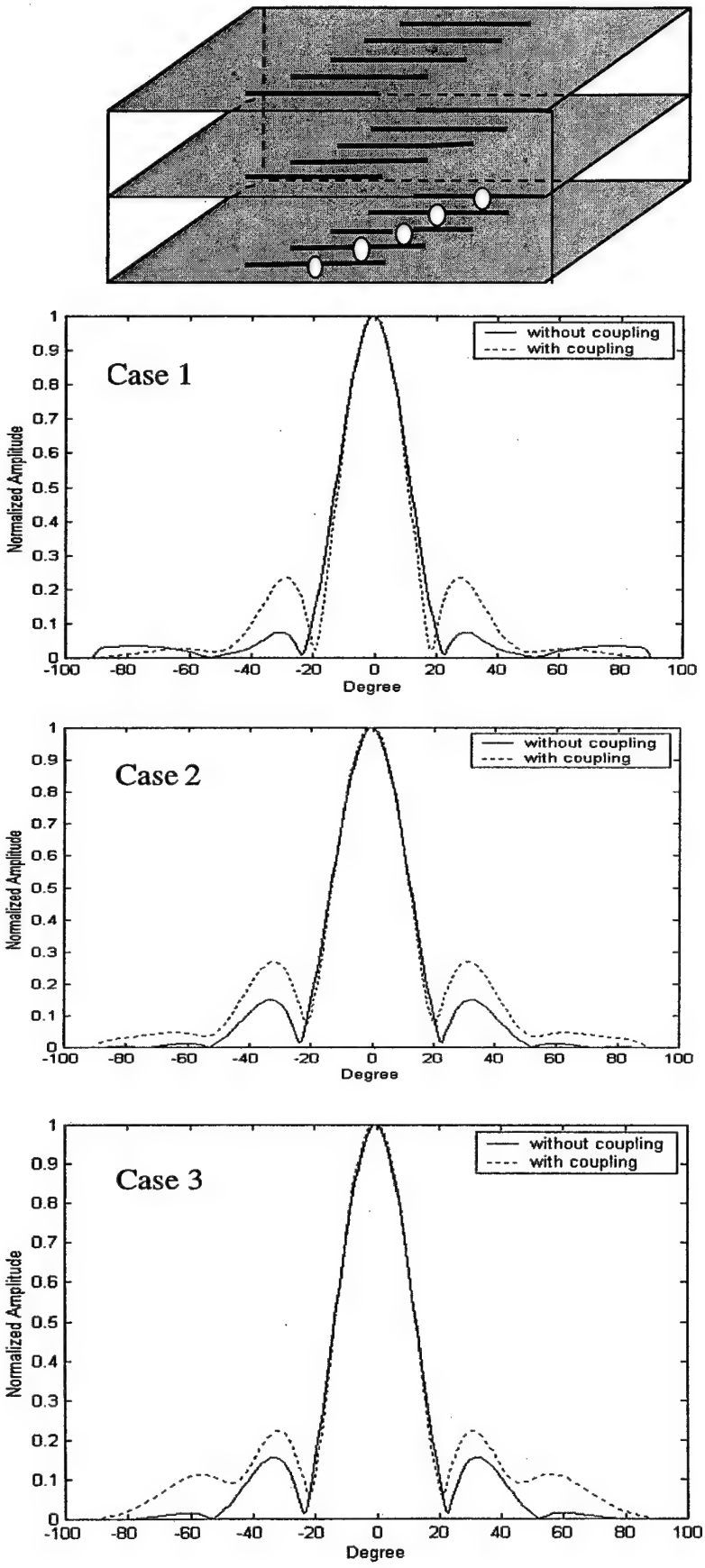

Figure 7: Patterns in the $\phi = 90°$ plane for a 5-element side-by-side array of Yagi-like antennas

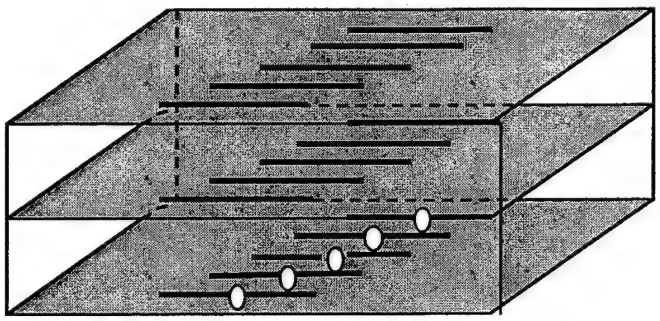

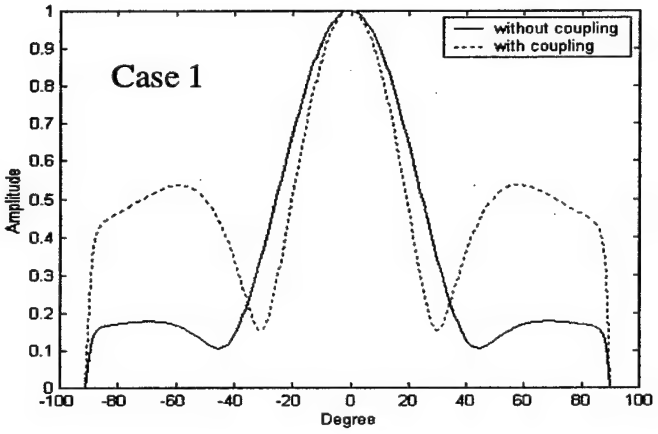

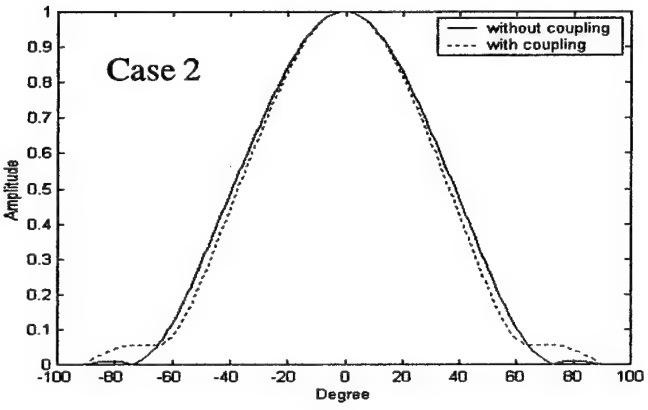

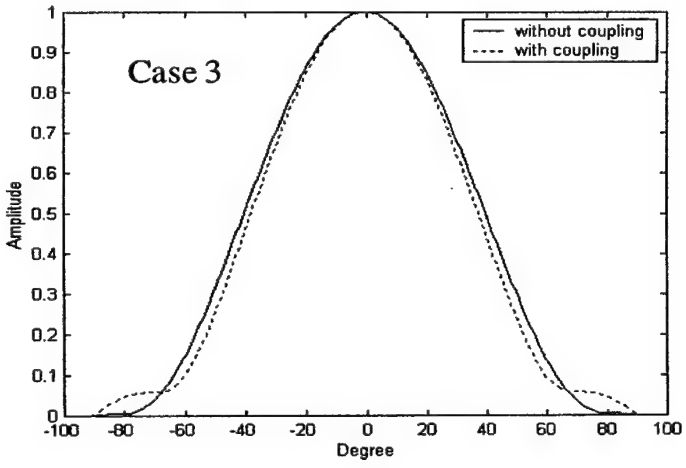

Figure 8: Patterns in the $\phi = 0$ plane for a 5-element side-by-side array of Yagi-like antennas

III. AN ELECTROMAGNETIC OTIMIZATION ENGINE FOR MULTI-LAYER PRINTED ANTENNA STRUCTURES

Designs of low profile, planar and conformal antennas in a multi-layered substrate environment are rapidly becoming of increasing importance in many radar and communication applications. Examples include, design of stacked patch antennas for broadband or multiple-frequency, dual-polarized and high gain applications. To optimize and design these antenna structures, an efficient numerical engine for electromagnetic modeling together with multi-objective / multi-parameter global optimization capabilities is needed. There is no treatment of a general multiply stacked multiple patches (MSMP) in open literature though theoretical and experimental analyses of stacked patches in a two-layer microstrip configuration or multiple patches on a single-layer microstrip substrate are available. On the other hand, several proprietary software packages such as Ensemble [4] and IE3D [5] can be utilized for analysis but not for optimal design.

In this work, we have developed an optimization and design engine which uses a hybrid combination of the method of moments (MOM) and evolutionary programming (EP) to globally optimize a given MSMP antenna structure.

A. Implementation of the Method of Moments

We have used the mixed-potential integral equation (MPIE)[6,7] to model planar microstrip structures of arbitrary shape in a multi-layered dielectric medium (Figure 9). For $P(m)$ patches on mth layer as shown in Fig. 9, there are $P(m)$ MPIE's in the following form (p=1, 2, …, $P(m)$):

$$-\frac{j\eta_0 k_0^2}{2\pi}\sum_{n=1}^{N}\sum_{q=1}^{Q(n)}\iint_{S_{nq}}\left[G^{M}_{mp,nq}(\mathbf{r}\,|\,\mathbf{r}')\mathbf{J}_{nq}(\mathbf{r}')+\frac{1}{k_0^2}\nabla G^{E}_{mp,nq}(\mathbf{r}\,|\,\mathbf{r}')\nabla'\cdot\mathbf{J}_{nq}(\mathbf{r}')\right]dS'-Z_{mp}\mathbf{J}_{mp}(\mathbf{r})=-\mathbf{E}^{i}_{mp}(\mathbf{r}) \qquad (1)$$

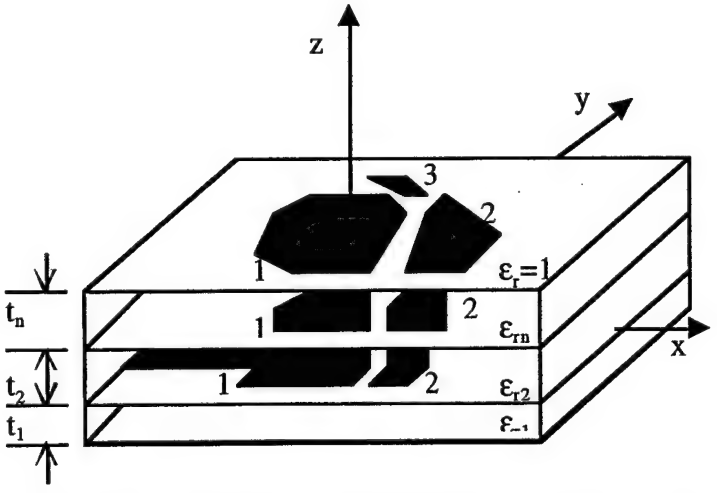

Figure 9: A multi-layered microstrip antenna structure

In (1), $\mathbf{J}_{mp}$ and Z_{mp} are the electric surface current and the surface impedance of pth patch on mth layer, respectively. $\mathbf{E}^{i}_{mp}$ is the excited tangential electric field on that patch. For the present problem, it is assumed that an ideal voltage gap generator is connected to the feed at the truncated end. $G^{M}_{mp,nq}$ and $G^{E}_{mp,nq}$ are the scalar Green's functions of electric and magnetic types, evaluated at pth patch on mth layer due to a source at qth patch on nth layer. These functions, which are of the Sommerfeld type and exhibit a translational invariance along x and y, can be pre-computed for a range of lateral distance. Our implementation of the MPIE utilizes a novel technique for a semi-analytical evaluation of these Green's functions and is, therefore, well suited for a medium with many dielectric layers [1,8]. In total, there are $P(1)+P(2)+\cdots+P(N)$ equations like (1).

To solve the equations for the unknown surface current, moment method with Galerkin's testing procedure has been used. The process begins with the following expansion of the x- and y-current into rooftop basis functions in x- and y-direction,

$$\mathbf{J}_{nq}(\mathbf{r}') = \hat{\mathbf{x}} \sum_{u=1}^{U(nq)} I_{nq}(u) B^{x}_{nq}(x'-x_{nq,u}) + \hat{\mathbf{y}} \sum_{v=1}^{V(nq)} I_{nq}(U+v) B^{y}_{nq}(y'-y_{nq,v}) \qquad (2)$$

where $I_{nq}(u)$ and $I_{nq}(U+v)$ are the coefficients of the basis functions B^{x}_{nq} and B^{y}_{nq}, respectively. Testing the equation for pth patch on mth layer using $\hat{\mathbf{x}} B^{x}_{mp}(x-x_{mp,u})$ (u=1, 2, ..., U) and $\hat{\mathbf{y}} B^{y}_{mp}(y-y_{mp,v})$ (v=1, 2, ..., V) in order, will generate $U(mp)+V(mp)$ equations. In such a way, testing every equation for the corresponding patch results in $\sum_{m=1}^{N} \sum_{p=1}^{P(m)} [U(mp)+V(mp)]$ equations with unknowns coefficients of the same number. In matrix form, we have $\mathbf{AI} = \mathbf{C}$ where $\mathbf{A}$ is a square matrix (usually called impedance matrix), $\mathbf{I}$ and $\mathbf{C}$ are column matrices respectively containing the coefficients of the current expansion functions and excitations. A typical matrix solver like LU algorithm can be used to solve for $\mathbf{I}$.

Once the coefficients of the current expansion functions are obtained, all patch currents including the one on the feed can be calculated using (2). A de-embedding scheme similar to the one in [7] can then be used to obtain the voltage reflection coefficient and as a result the input impedance Z_{in}. The total radiated far-fields of the structure can also be obtained by integration of the current distributions, weighted by the far-field natural modes, over the surface of the conducting patches. For the sake of brevity the details are not included in this report.

A.1. Verification of the Moment-Method Code

To verify our developed code, we first simulate a single-layer patch antenna using our own code and Ensemble. The patch is a rectangular one operating at 7.5 GHz and its dimensions are

15.8114×12.7712 mm^2. The substrate thickness is 0.79375 mm. The relative dielectric constant and loss tangent of the substrate are 2.2 and 0.001. The feed line is 2.46467-mm wide and feeds the patch (along a radiating edge) at a distance of 3.991 mm from a non-radiating edge. Figure 10(a) and (b) show respectively the real and imaginary parts of the normalized input impedance in comparison. Figure 11 compares the return loss data from the two codes. It is seen that our data are in good agreement with those from Ensemble except for a frequency shift of 0.3%.

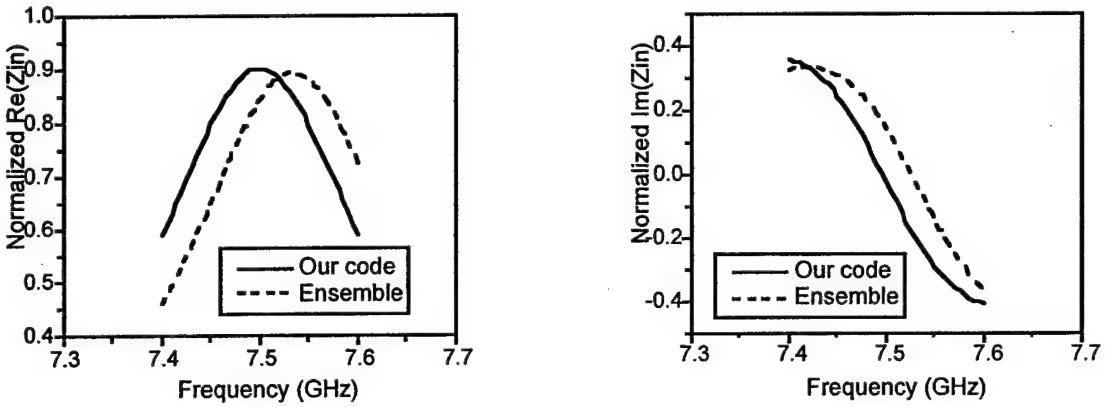

Fig. 10: The real and imaginary parts of the normalized input impedance of a single patch antenna.

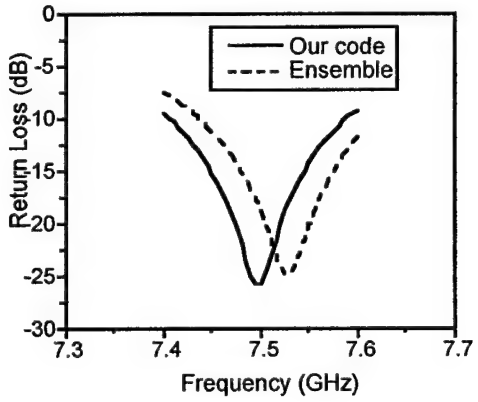

Figure 11: Return loss of the patch antenna

The second example is simulation of stacked patches in a two-layer media. This structure was modeled and measured by Dubost and Beauquet [9]. The first patch of dimensions 6.4×6.4 mm^2 is fed at the center of an edge by a 0.6-mm wide microstrip line and printed on the first lossless substrate with ε_{r1}=2.55 and t_1=0.8 mm. The second patch of dimensions 5.6×5.6 mm^2 is printed on the second substrate with ε_{r2}=2.55 and t_2=1.6 mm and arranged symmetrically with its sides parallel to those of the first patch. The real and imaginary parts of the normalized input impedance of the

antenna structure from the two codes are shown in Figure 12(a) and (b) for comparison. In Figure 13, the return loss data from the codes are compared with the measured ones from literature. Again, a good agreement between the data from our code and those from Ensemble is observed. Also, both sets of simulated return loss data exhibit accordance with the measured ones. This stacked-patch antenna is actually a broadband example. Our calculated and Dubost's measured bandwidths (VSWR=2) are 13.1% and 13.5%, respectively.

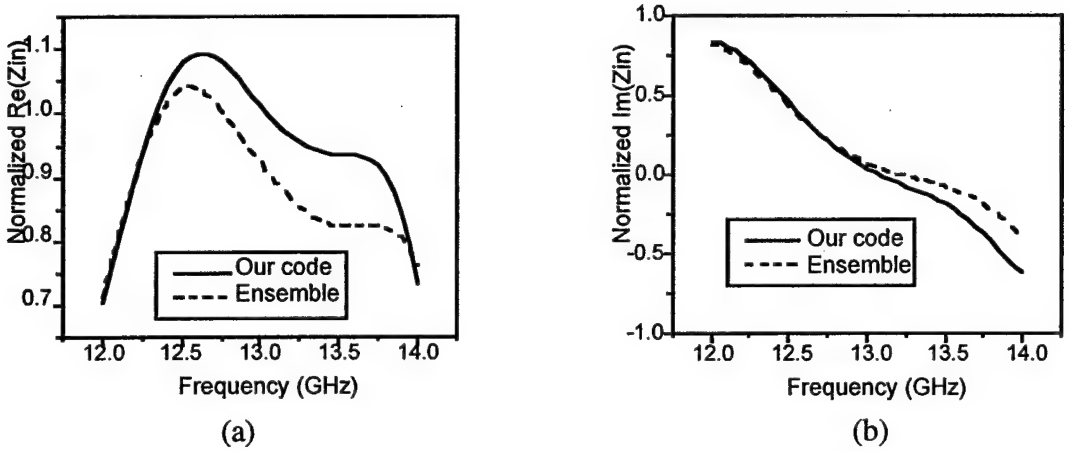

Fig. 12: The real and imaginary parts of the normalized input impedance of a stacked-patch antenna.

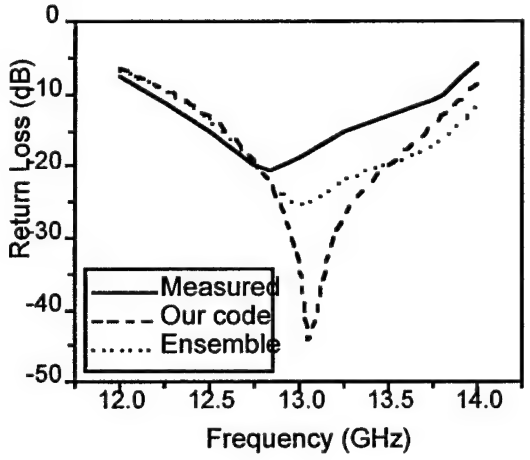

Figure 13: Simulated return loss in comparison with measured data by Dubost and Beauquet

B. Implementation of the Evolutionary Programming

Evolutionary programming (EP) [10] is well suited for global optimization of continuous, discrete, and mixed parameter problems that one may often encounter in electromagnetics and antenna design. Like other evolutionary computational techniques, such as GA [11] and ES [12],

EP is a heuristic population-based search procedure that incorporates random variation and selection. However, whereas GA uses a combination of crossover and mutation with the former being the main mechanism of change, EP uses mutation as the only variation operator. The mutation only nature of EP may provide a powerful tool in design of the problem specific operators and facilitate easy integration with available apriori knowledge about a given problem. We have experimented with two different mutation operators, namely Gaussian and Cauchy, in the optimization module of our electromagnetic optimization engine. In this part, we first present the details of two modified EP algorithms: meta-EP with Gaussian mutation, and Fast Evolutionary Programming (FEP) with Cauchy mutation. These algorithms combine the mutation-based evolution of EP with the self-adaptation of the strategy parameters in ES. The algorithms are then applied to the challenging constrained optimization problem of the printed Yagi-like array of stacked dipoles.

B.1. Algorithms for meta-EP and FEP

The EP algorithm with self-adaptive mutation operator for global optimization of an n-dimensional objective function $\phi(\bar{x})$, $\bar{x} = [x(1), x(2), \ldots, x(n)]$ consists of five basic steps: initialization, fitness evaluation, mutation, tournament and selection.

Initialization: An initial population of μ individuals is formed through a uniform random or a biased distribution. Each individual is taken as a pair of real-valued vectors, $(\bar{x}_i, \bar{\eta}_i)$, $\forall i \in \{1, \ldots \mu\}$ where $\bar{x}_i = [x_i(1), x_i(2), \ldots, x_i(n)]$ and $\bar{\eta}_i$ are the n-dimensional solution and its corresponding strategy parameter (variance) vectors, respectively. $\bar{\eta}_i$'s are initialized based on the user-specified search domains, $\bar{x}_i \in \{x_{min}, x_{max}\}^n$, which may be imposed at this stage.

Fitness Evaluation: A fitness function $F(\bar{x}_i)$ is assigned to each vector $\bar{x}_i$ in the population. $F(\bar{x})$ in general is obtained from the objective function $\phi(\bar{x})$ by possibly imposing some random alteration β and the scaling them back to negative real values by a scaling function α,

$$F(\bar{x}) = \alpha(\phi(\bar{x}), \beta) + P(\bar{x}) \qquad (3)$$

where P is a collection of penalty criteria assigned to possible optimization constraints.

Mutation: In EP, mutation is the only variation operator used for generation of offsprings population from the parents population, and therefore EP, in contrasts to Gas, is asexual by nature, i.e., each single parent produces one single offspring. Design of efficient mutation operators is presently an ongoing topic of research in evolutionary computation. Here we present two algorithms, meat-EP [12,13] and Fast Evolutionary Programming (FEP)[14], which use different

mutation operators in the evolution process. In meta-EP, each parent $(\bar{x}_i, \bar{\eta}_i)$ creates a single offspring $(\bar{x}_i', \bar{\eta}_i')$ by:

$$x_i'(j) = x_i(j) + \sqrt{\eta_i(j)}\, N_j(0,1) \tag{4}$$

$$\eta_i'(j) = \eta_i(j)\, e^{[\tau' N(0,1) + \tau N_j(0,1)]} \tag{5}$$

for j = 0,1,2,....n, where $x(j)$ and $\eta(j)$ and are the jth components of the solution vector and the variance vector, respectively. N(0,1) denotes a one-dimensional random variable with a Gaussian distribution of mean zero and standard deviation one. Nj(0,1) indicates that the random variable is generated anew for each value of j. The scale factors τ and τ' are commonly set to $\left(\sqrt{2\sqrt{n}}\right)^{-1}$ and $\left(\sqrt{2n}\right)^{-1}$, respectively, where n is the dimension of the search space. Self-adaptive mechanism of equation (5), borrowed from ES, enables the meta-EP to evolve its own variance parameters during the search, exploiting an implicit link between internal model and good fitness values. The logarithmic normally distributed process for the variances in (5) guarantees positive values of standard deviations. The global factor τ' N(0,1) allows for an overall change of mutability and guarantees the preservation of all degrees of freedom, whereas the factor τ Nj(0,1) allows for individual changes of the variances η(j).

In FEP algorithm the offsprings are still generated according to the equations (4)-(5), but with a Cauchy mutation operator replacing the Gaussian mutation in (4), i.e.,

$$x_i'(j) = x_i(j) + \sqrt{\eta_i(j)}\, C_j(0,1) \tag{6}$$

where C(0,1) is a random variable with a Cauchy distribution operator, G, centered at the origin and with the scale parameter t = 1,

$$G_t(x) = \frac{1}{2} + \frac{1}{\pi}\tan^{-1}\left(\frac{x}{t}\right) \quad ; \quad -\infty < x < \infty \tag{7}$$

We note that the inverse of the operator in (7), needed in generation of the random variables in (6), is given in closed form. It has been shown that FEP performs much better than EP using the Gaussian mutations for many unconstrained optimizations involving multimodal functions with many local minima as well as in nonlinear signal processing.

Tournament: In tournament process a pairwise comparison with respect to the fitness values in (3) over the union of parents and offspring populations is conducted. For each individual $\bar{a}_k$ in the union, $k \in \{1,.... 2\mu\}$, q opponents are chosen at random with equal probability from the total

membership 2μ of the union. For each comparison, if the individual fitness $F(\bar{a}_k)$ is no greater than the opponent's, it receives a "win". The best individual is guaranteed a maximum 'win' score of q and its survival to the next generation. We note that this tournament process differs from the one in Gas and is 'elitist' in nature.

Selection: The μ individuals out of the union of $(\bar{x}_i, \bar{\eta}_i) \cup (\bar{x}_i', \bar{\eta}_i'), \forall i \in \{1, \ldots 2\mu\}$ with the most "win" score are selected to be the parents of the next generation. The above steps in the fitness evaluation through the selection process is then repeated until an acceptable solution is obtained or the prescribed total number of generations is reached.

Figure 14 shows the flow chart of our electromagnetic optimization engine.

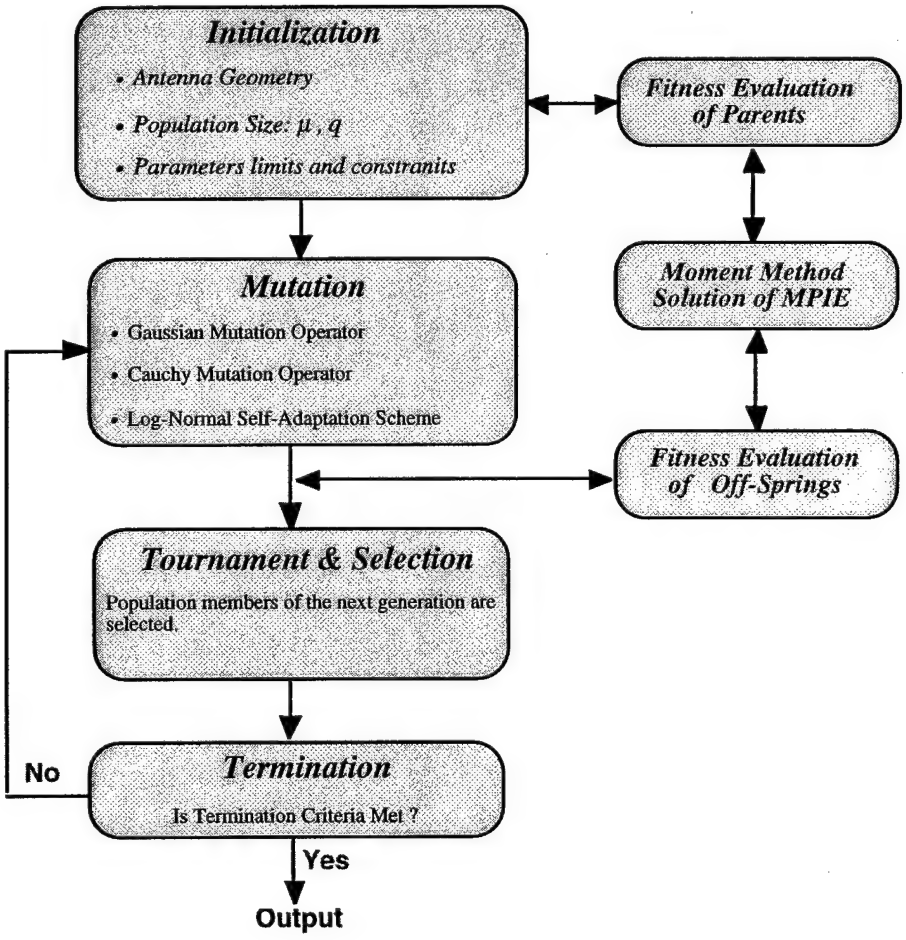

Figure 14: An Electromagnetic Optimization Engine for Multi-layered Printed Antenna Structures

C. Examples of Gain Optimization of the Yagi-Like Antennas

To optimize the gain, the Yagi-like structure is represented as a vector consisting of the length of the driver element, the director lengths, the relative permittivity and the dielectric thickness as given below:

$$\overline{X} = [L_{dri},\ L_{dir}(1),...,L_{dir}(N),\ \varepsilon_r(1),...,\varepsilon_r(N),\ dl(1),...,dl(N)]^T \tag{8}$$

where L_{dri} and $L_{dir}(i)$, $\varepsilon_r(i)$ and dl(i) are length of the driver element, length of the ith director element, dielectric constant and thickness of the ith dielectric layer, respectively. Length of the vector in (8), in view of the mutations (4)-(5), is in general n = 6N+1. For the gain optimization we construct the Fitness function in (3) with $\alpha = -1$ and $\beta = 0$,

$$F(\overline{x}) = -\ Gain(\theta,\ \phi;\ \overline{x}) + \sum_m P_m(\overline{x}) \tag{9}$$

where *Gain* is the power gain in $(\theta,\ \phi)$ direction obtained from the moment method solution of a mixed-potential integral equation for the current distributions on the strip elements; P_m , m = 1,2,.., are the penalty criteria for violating a set of constraints chosen to ensure that the optimized solutions are practically feasible.

In the first example, we present the performances of the EP and FEP algorithms in an unconstrained optimization of a five layer Yagi array with air dielectric layers. The population size and the number of opponents were set to μ = 100 and q = 10, respectively. Optimization was performed with respect to lengths of the elements and thickness of the layers. Figure 15 shows the mean fitness-value trajectory of the best population member at each generation after 5 trial runs were performed. As seen FEP performs better than meta-EP in terms of convergence rate. A gain of better than 17dBi was obtained after 155 generations.

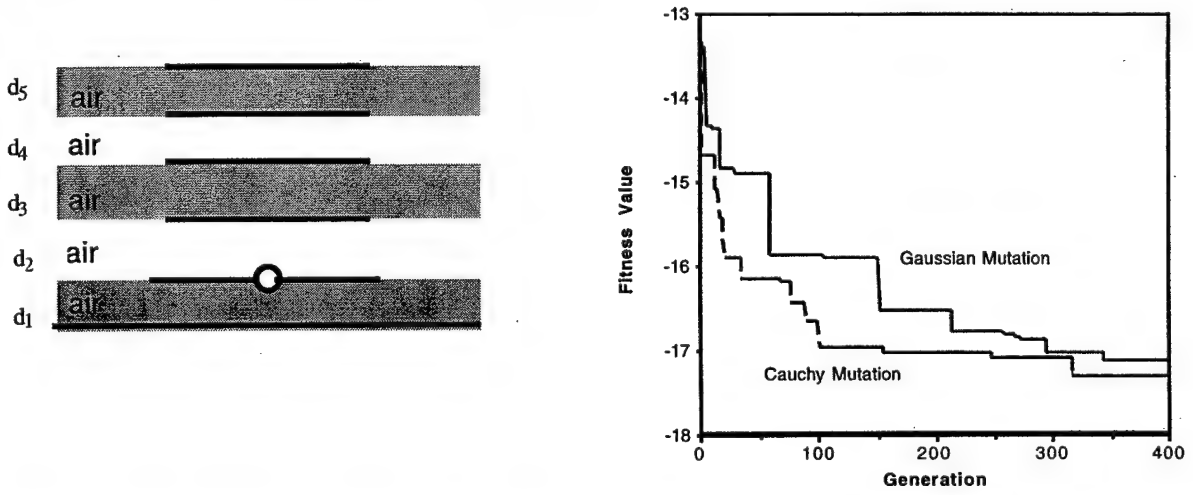

Figure 15: Optimization of a 5-layer printed Yagi antenna with air dielectric using two mutation operators

In the second example, a Yagi-like array in a 3 layer isotropic medium was optimized with μ = 20, q = 8 and subject to the constraints of $D = d_1+d_2+d_3 < 0.15\lambda_0$ and radiation efficiency, e_s > 95%. The optimization parameters in this case were lengths of the elements, thickness of the layers and the dielectric constants, which were allowed to vary in the range of 2 to 4. It was observed that ε_{r1} and ε_{r2} always tended to 2 while ε_{r3} tended to 4; this is consistent with the high gain condition for an embedded dipole [2]. The corresponding mean fitness trajectories for meta-EP and FEP after 5 trials are plotted in Figure 16. Meta-EP performs better than FEP for this constrained optimization case. Gain of about 13 dBi with $D = 0.12\ \lambda_0$ and e_s = 99% was obtained within 200 generations. It is noteworthy that the same structure without the director elements has a gain of only about 7.5 dBi. Gain and surface-wave powers of this structure are plotted as a function of normalized frequency in Figure 17. As can be seen at the maximum gain, the power coupled into the surface waves is minimized.

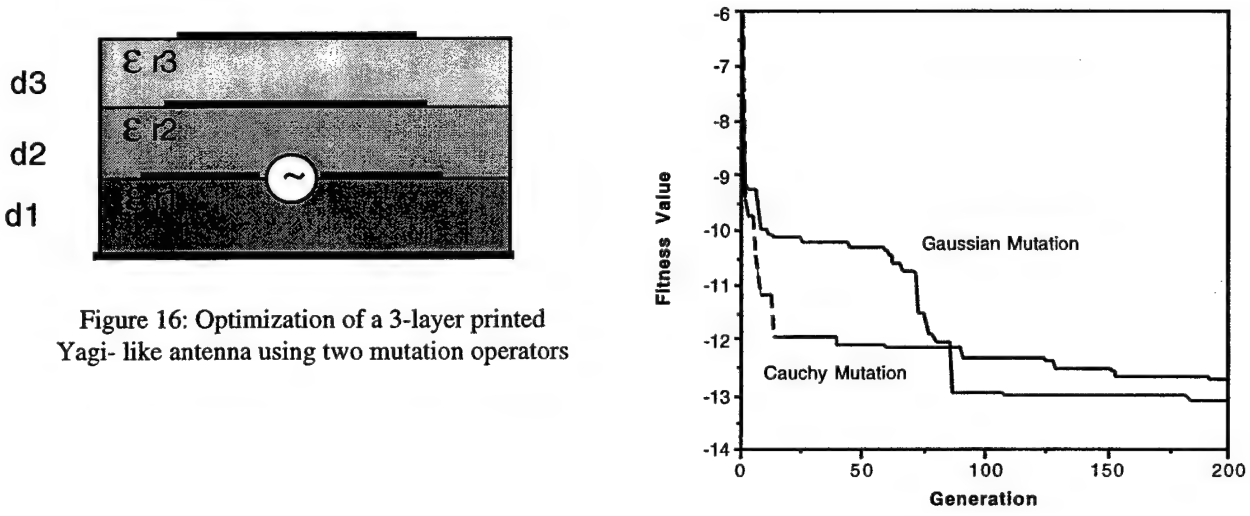

Figure 16: Optimization of a 3-layer printed Yagi- like antenna using two mutation operators

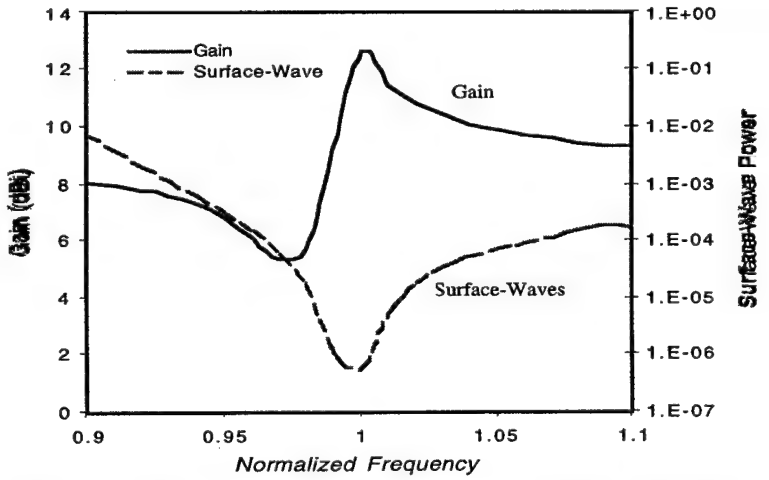

Figure 17: Gain and surface-wave power versus normalized frequency

IV. DESIGN OF HIGH GAIN CIRCULARLY POLARIZED MICROSTRIP PATCH ANTENNAS

In order to demonstrate the design feasibility of multi-layer high gain microstrip antennas for circular polarization (CP) applications, a three-layer rectangular patch antenna is designed for MSAT operation. The specifications require a gain of larger than 10 dBi with an axial ratio (AR) of less than 1 dB at a center frequency of f=1.643 GHz.

A. Design Procedure

We have used a nearly square patch fed by a coaxial line along its diagonal as shown in Figure 18. For a Duroid substrate with $\varepsilon_{r1} = 2.2$ and $d_1 = 1.59$ mm, the dimensions L and W of the patch were initially selected for CP according to [15]: $L = W\ (1+1/Q_t)$ where Q_t is the total quality factor of patch. Using a MOM-based simulation code, the feed position was then optimized, in the absence of any superstrate layer, until a low VSWR was achieved. Figure 18 shows the axial ratio, gain and return- loss (S11) of the initial design. At the frequency of 1.643 GHz, AR = 0.278 dB and VSWR = 1.2. The realized gain, however, is only about 7.1 dBi. In order to enhance the gain, a high permittivity superstrate layer of thickness d_3 is added at a distance of d2 from the patch surface as shown in Figure 19. A high gain pattern can now be obtained by adjusting the thickness d_2 when d_3 is fixed according to the resonance condition [2]: $d_3 = \lambda_0 / 4\sqrt{\varepsilon_{r3}}$. It is noteworthy that the presence of the air layer allows an easy mechanical tuning of d_2 in a practical design [16]. Resonance frequency of the original patch shifts, however, when the superstrate layers are added which hence requires adjustments of the patch dimensions and the feed position. After many simulation trials, we have finally achieved a realized gain of about 11.68 dBi with an axial ratio of AR=1.08 dB and VSWR of 1.25 at f=1.643 GHz. The antenna performance as a function of frequency together with the final design parameters is shown in Figure 19.

B. Performance of the Designed Antenna in a Linear Array Environment

It may be desirable to also form an array of such high gain antenna elements for even higher gain, low side lobe and/or steered-beam applications. Since these elements have relatively thick dielectric layers, propagation of surface-waves and strong mutual couplings may adversely affect the gain, axial ratio and input impedance of these antennas. To investigate the coupling effects we have analyzed a two-element array of the above three-layer design. Figures 20-a and 20-b show the gain and axial ratio of the array for the E-plane coupling (i.e., when the elements' W sides are facing each other) and the H-plane coupling (i.e., when the elements' L sides are facing each other), respectively. As can be seen, for a typical 0.5 λ_0 spacing, the axial ratio has degraded from 1.08 dB for an element in isolation to more than 5 dB for the array. Therefore, for these multi-layered configurations, one needs to optimize the whole array for both high gain and low axial ratio.

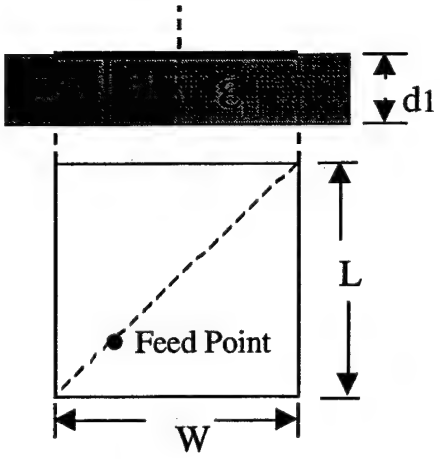

L=60 mm, W=60.79 mm

x_0=40.1 mm, d1=1.5875 mm

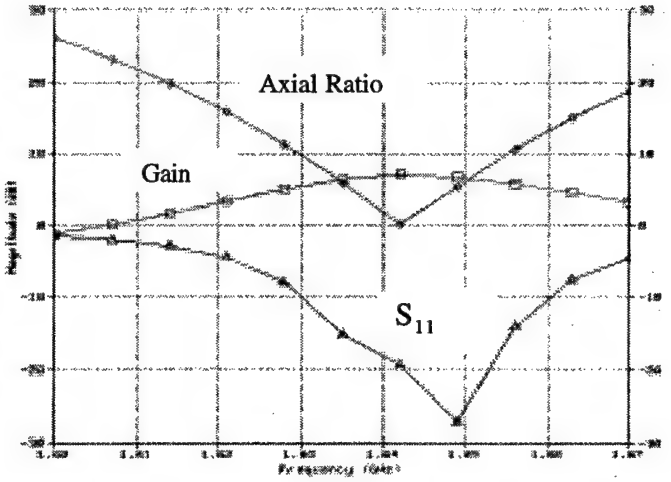

Figure 18: Axial ratio, gain and return loss of a single layer CP microstrip patch antenna

L=59.7 mm, W=60.52 mm

x_0=39.6 mm, d1=1.5875 mm

d2=77 mm, d3=24.5 mm

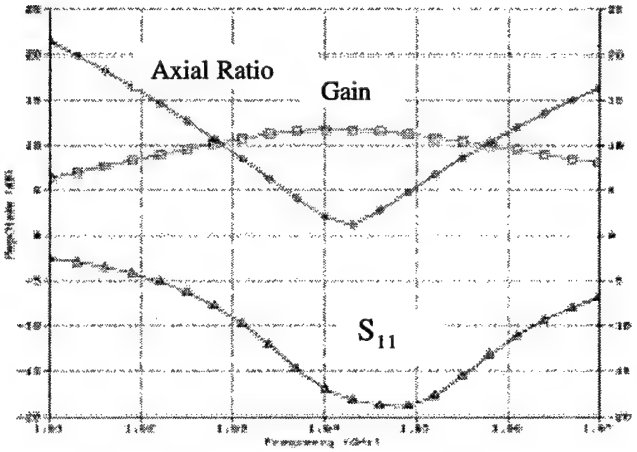

Figure 19: Axial ratio, gain and return loss of a 3-layer high gain CP microstrip patch antenna

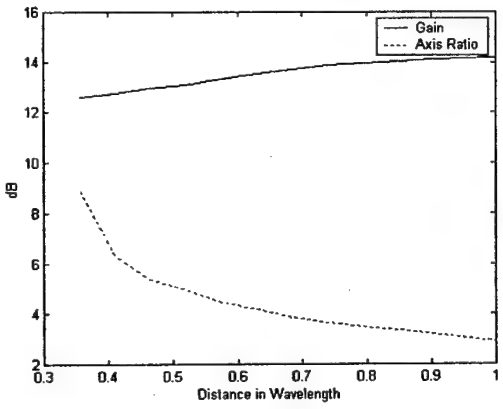

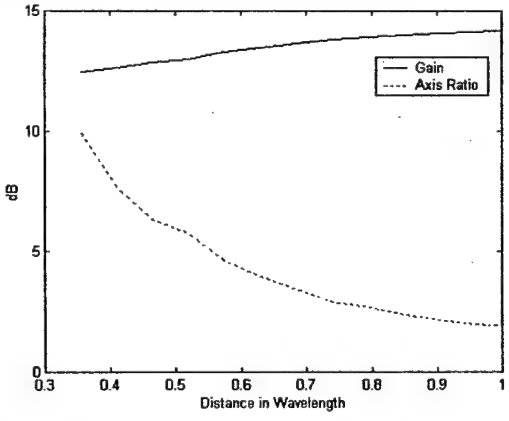

(a) (b)

Figure 20: Effects of mutual coupling on the gain and the axial ratio of the array.
(a): E-plane coupling; (b):H-plane coupling

V. GAIN ENHANCEMENT METHOD FOR MICROSTRIP ANTENNAS IN UNIAXIAL ANISOTROPIC MEDIA

As a first step toward the extension of the Yagi-like concept to antennas printed in multi-layer anisotropic media, we have analyzed the conditions for obtaining high gain together with high radiation efficiency for a microstrip dipole antenna embedded in a multi-layer anisotropic medium.

A. Analysis of High Gain Conditions

The conditions for obtaining high gain from an embedded dipole in a multi-layered isotropic medium have been discussed in [2, 3] where it was shown that it is possible to obtain very high gain by alternating between high wave-impedance (large μ_r) and low-wave impedance (large ε_r) layers. In this work we have extended the above gain enhancement method to the case of a microstrip dipole printed in a multi-layered uniaxial anisotropic medium with permittivity and permeability dyadics of (Figure 21)

$$\bar{\bar{\varepsilon}}_n = \begin{pmatrix} \varepsilon_{tn} & 0 & 0 \\ 0 & \varepsilon_{tn} & 0 \\ 0 & 0 & \varepsilon_{zn} \end{pmatrix} = \bar{\bar{I}}_t\, \varepsilon_{tn} + \hat{z}\,\hat{z}\, \varepsilon_{zn} \quad ; \quad \bar{\bar{\mu}}_n = \begin{pmatrix} \mu_{tn} & 0 & 0 \\ 0 & \mu_{tn} & 0 \\ 0 & 0 & \mu_{zn} \end{pmatrix} = \bar{\bar{I}}_t\, \mu_{tn} + \hat{z}\,\hat{z}\, \mu_{zn} \qquad (10)$$

By using an equivalent cascaded transmission line method, explicit expressions for the corresponding far-fields were derived and the conditions of obtaining high gain together with high radiation efficiency (i.e., ratio of the radiated power to the total of the radiated plus the surface-wave powers) were analyzed. In particular, we have shown that by a proper selection of anisotropy ratios and thickness of the layers, it is possible to obtain two beams at θ_E and θ_H in E and H planes respectively. More explicitly, for the case of a three layer structure in Figure 21, with $\bar{\bar{\varepsilon}}_1 = \bar{\bar{\varepsilon}}_2$, $\bar{\bar{\mu}}_1 = \bar{\bar{\mu}}_2$, the high gain conditions are derived as:

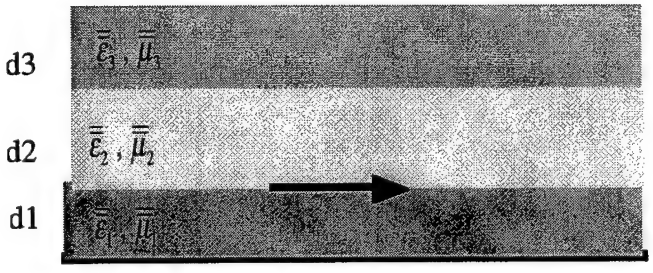

Figure 21: A Microstrip Dipole in a Multi-layered Uniaxial Medium

$$\sqrt{\frac{\mu_{zn}}{\mu_{tn}}}\sin(\theta_E)=\sqrt{\frac{\varepsilon_{zn}}{\varepsilon_{tn}}}\sin(\theta_H) \tag{11}$$

$$d_1=d_2=\frac{\lambda_0}{4n_{t1}}\left[1-\frac{\sin^2(\theta_E)}{\mu_{t1}\varepsilon_{z1}}\right]^{-\frac{1}{2}} \quad ; \quad d_3=\frac{\lambda_0}{4n_{t3}}\left[1-\frac{\sin^2(\theta_E)}{\mu_{t3}\varepsilon_{z3}}\right]^{-\frac{1}{2}} \tag{12}$$

In general, the condition in (11) has to be satisfied for each uniaxial layer in order to generate two beams exactly in θ_E and θ_H directions. One, however, can still obtain two beams approximately at θ_E and θ_H if only the first two layers satisfy (11). In that case the third layer can be either anisotropic or isotropic. More specifically, for the case of nonmagnetic layers the high gain conditions can be reduced to,

$$d_{1,2}=\frac{\sqrt{\varepsilon_{z1}}\,\lambda_0}{4\sqrt{\varepsilon_{t1}}\sqrt{\varepsilon_{z1}-\sin^2\theta_E}} \quad ; \quad d_3=\frac{\lambda_0}{4\sqrt{\varepsilon_{t3}}} \quad ; \quad \sqrt{\varepsilon_{t1}}\sin(\theta_E)=\sqrt{\varepsilon_{z1}}\sin(\theta_H) \tag{13}$$

which together with $\varepsilon_{t3} >> 1$ produce two high gain beams. Aside from a normalization factor, the corresponding far-fields, approximated near the main beams in the θ_E and θ_H directions, are given by:

$$\left|E_\theta\right|^2 \cong \frac{\frac{\varepsilon_{t3}}{\varepsilon_{t1}}\cos^4(\theta_E)\left(1-\frac{\sin^2(\theta_E)}{\varepsilon_{z1}}\right)}{1+\left[2kd_1\frac{\varepsilon_{t3}}{\varepsilon_{z1}}\cos^2(\theta_E)\sin(\theta_E)\right]^2(\theta-\theta_E)^2} \tag{14}$$

$$\left|E_\phi\right|^2 \cong \frac{\frac{\varepsilon_{t3}}{\varepsilon_{t1}\left(1-\frac{\sin^2(\theta_H)}{\varepsilon_{z1}}\right)}}{1+\left[\frac{2kd_1\varepsilon_{z3}}{\varepsilon_{z1}-\sin^2(\theta_H)}\right]^2(\theta-\theta_H)^2} \tag{15}$$

These expressions clearly show that for $\varepsilon_{tr3} / \varepsilon_{tr1} >> 1$, E_θ and E_ϕ provide two beams at θ_E and θ_H, respectively.

The above formulation is valid for an infinitesimal printed Hertzian dipole. In order to analyze resonant or other finite-length printed dipoles in multi-layered uniaxial media, the moment-method based MPIE code was extended to include uniaxial layers by modifying the corresponding Green's functions. We also plan to extend the code to patch antennas of arbitrary shapes.

B. Numerical Results

For $\theta_E = 60°$ and $\theta_H = 30°$ one requires, say, $\varepsilon_{z1} = \varepsilon_{z2} = 3$ and $\varepsilon_{t1} = \varepsilon_{t2} = 1$. Setting the third layer to be isotropic with $\varepsilon_{t3} = \varepsilon_{z3} = 26$, then results in gains of about 17.1 dBi in H-plane and about 9 dBi in E-plane together with a radiation efficiency of 80% for a nearly resonant strip dipole of length 104 mm at f= 1 GHz.. The input impedance is $Z_{in} = 154 - j40$ ohms. The corresponding patterns are shown in Figure 22-a. The minor beam pointing error in the E-plane pattern is because the equation (11) is not satisfied for the third layer. The gains can be increased by increasing the number of isotropic layers and alternating between high and low dielectric constants according to the resonant conditions in [3, 17]. Figure 22-b shows the patterns for a five layer case with two anisotropic layers with $\varepsilon_{z1} = \varepsilon_{z2} = 3$ and $\varepsilon_{t1} = \varepsilon_{t2} = 1$, and three isotropic layers with $\varepsilon_{r3} = 26$, $\varepsilon_{r3} = 2$ and $\varepsilon_{r3} = 26$. Gains of 22.4 dBi in H-plane and 17.1 dBi in E-plane together with a radiation efficiency of 98% are obtained. The input impedance in this case is $Z_{in} = 141 - j46$ ohms.

Finally, we have shown that, similar to the isotropic case previously reported in the literature [18], the primary radiation mechanism in the uniaxial case is also the leaky-wave excitation. Details of this analysis will be reported in the next annual report.

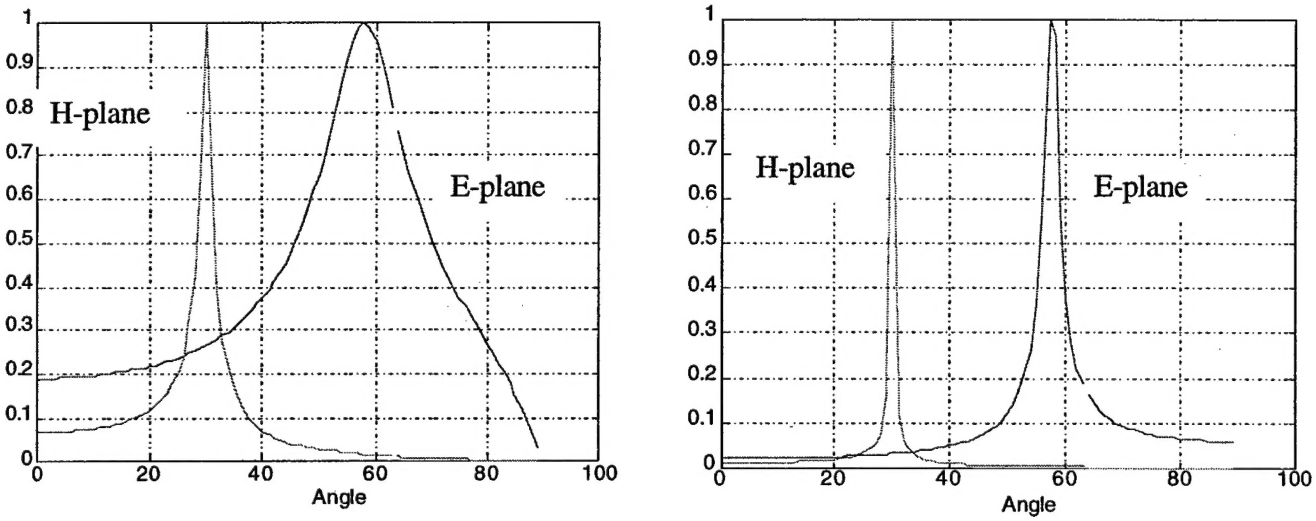

(a) (b)

Figure 21: Normalized far-field patterns of a near resonant microstrip dipole antenna. (a): antenna embedded in a 3-layer uniaxial medium; (b): antenna embedded in a 5-layer uniaxial medium.

VI. FUTURE WORKS

Our research works on the multi-layered printed antennas that are either presently in progress or are planned for the 1999-2000 academic year include the followings:

- We are presently in the midst of applying our electromagnetic optimization engine for gain optimization of microstrip line-fed Yagi-like patch antennas and arrays for linear as well as circular polarization. Other configurations planned for optimizations include proximity-coupled-fed and coaxial-fed microstrip patch antennas. We also plan to fabricate and experimentally verify selected optimized designs for such applications as in GPS and/or MSAT.

- We plan to use our electromagnetic optimization engine to develop novel schemes for shape optimization of printed antennas for various multi-function applications such as multi-band, wide-band and/or multi-polarization operations. We also plan to fabricate and measure a few shaped-optimized microstrip antennas in order to validate any novel design concepts, which may result from this investigation.

- We plan to extend our electromagnetic optimization engine to include Yagi-like stacked patch antennas printed in a multi-layer anisotropic medium. The optimization engine will then be used to investigate these antennas for high gain multi-beam applications.

- We plan to analyze the Yagi-like antennas in terms of the leaky-wave excitation in order to better understand the physics of their high gain radiation. The analysis will be performed for both isotropic as well as uniaxial anisotropic cases.

REFERENCES

[1] A. Hoorfar, "Investigation of a new class of multi-layered printed antennas for applications in communications and radar," Annual Report submitted to ONR, October 1998.

[2] D. R. Jackson and N. G. Alexopoulos, "Gain enhancement methods for printed circuit antennas", *IEEE Trans. Antennas Propagat.*, Vol. AP-33, pp. 976-987, Sept. 1985.

[3] H. Y. Yang and N. G., Alexopoulos, "Gain enhancement technique for microstrip antennas," *IEEE Trans. Antennas Propagat.*, Vol. AP-35, pp. 860-863, July 1987.

[4] ENSEMBLE™ User's Guide, Ansoft Corporation, 1998.

[5] IE3D™ User's Manual, Zeland Software, Inc. 1997.

[6] J. R. Mosig, "Arbitrary shaped microstrip structures and their analysis with a mixed potential integral equation," *IEEE Trans. On Microwave Theory Tech.,* MTT-36, pp. 314 323, February 1988.

[7] D. C. Chang and J. X. Zheng, "Electromagnetic modeling of passive circuit elements in MMIC," *IEEE Trans. Microwave Theory Tech.*, vol. MTT-40, pp.1741-1747, Feb. 1992.

[8] A. Hoorfar and D. C. Chang, "Semi-analytical solutions for microstrip Green's functions in multi-layered media," *Proceedings of the 1998 International Symposium on Electromagnetic Theory*, pp. 618-620, May 1998, Thessaloniki, Greece.

[9] G. Dubost and G. Beauquet, "Patch antenna bandwidth increase by means of a director," *Electron. Lett.*, vol. 22, pp.1345-1347, 1986.

[10] D. B. Fogel, Evolutionary Computation: Toward a New Philosophy of Machine Intelligence, Piscataway, NJ: *IEEE Press*, 1994.

[11] D. E. Goldberg, Genetic Algorithms in Search, Optimization and Machine Learning, Reading, MA: *Addison Wesley*, 1989.

[12] T. Bäck, Evolutionary Algorithms in Theory and Practice, Oxford Univ. Press, 1996.

[13] K. Chellapilla and A. Hoorfar," Evolutionary programming: an efficient alternative to genetic algorithms for electromagnetic optimization problems," IEEE AP-S Int. Symp., June 1998.

[14] X. Yao and Y. Liu, "Fast evolutionary programming," Proc. of 5th Conf. on Evol. Prog., L. J. Fogel, P.I. Angeline, T. Bäck (editors), MIT Press, Cambridge, MA, 1996.

[15] C, A. Balanis, Antenna Theory, Analysis and Design, Wiley & Sons Inc., 2nd edition, 1997.

[16] X. H. Shen and A. E. Vandenbosch, "Study of gain enhancement method for microstrip antennas using moment method," *IEEE Trans. Antennas Propagat.*, Vol. AP-43, pp. 227-231, March 1995.

[17] A. Hoorfar, "Analysis of a 'Yagi-like' printed stacked dipole array for high gain applications," Microwave Opt.. Technol. Lett., pp. 317-321, April 1998.

[18] D. R. Jackson and A. A. Oliner, "A leaky-wave analysis of the high-gain printed antenna configuration," *IEEE Trans. Antennas Propagat.*, Vol. AP-36, pp. 905-910, July 1988.

REPORT DOCUMENTATION PAGE

Form Approved
OMB No. 0704-0188

1. AGENCY USE ONLY *(Leave blank)*	2. REPORT DATE	3. REPORT TYPE AND DATES COVERED
	October 22, 1999	Interim: October 1, 1998 - September 30, 1999

4. TITLE AND SUBTITLE
INVESTIGATION OF A NEW CLASS OF LOW-PROFILE MULTI-LAYER PRINTED ANTENNAS

5. FUNDING NUMBERS
G - N00014-98-1-0090

6. AUTHOR(S)
Ahmad Hoorfar

7. PERFORMING ORGANIZATION NAMES(S) AND ADDRESS(ES)
Villanova University
800 Lancaster Ave.
Villanova, PA 19085

8. PERFORMING ORGANIZATION REPORT NUMBER
Acc: 527615

9. SPONSORING / MONITORING AGENCY NAMES(S) AND ADDRESS(ES)
Office of Naval Research
Ballston Center Tower One
800 North Quincy Street
Arlington VA 22217-5660

10. SPONSORING / MONITORING AGENCY REPORT NUMBER

11. SUPPLEMENTARY NOTES

a. DISTRIBUTION / AVAILABILITY STATEMENT
Approved for Public Release: distribution is unlimited

12. DISTRIBUTION CODE

13. ABSTRACT *(Maximum 200 words)*

This progress report outlines our research efforts on modeling, analyses and optimization of multi-layered printed antennas for high gain applications. Our research during this interim period has resulted in progress in the following four areas. 1) Performance analysis of a linear array of Yagi-like printed sub-array antennas. Effects of mutual couplings on gain and pattern degradation of previously optimized Yagi-like structures are investigated for various array configurations. 2) Development of an electromagnetic optimization engine based on Method of Moments and Evolutionary Programming for design of multi-layer printed antennas. During this interim period, this code has been extended to include printed patch antennas of arbitrary shapes. In addition, the use of various mutation operators to speed-up the optimization process has been investigated in details where it has been found that a Cauchy mutation operator can significantly speed-up the optimal design of antenna structures. 3) Design of circularly polarized (CP) high gain multilayer antenna elements. The design feasibility of a high gain CP microstrip patch antenna is demonstrated for MSAT application where a gain of more than 11.6 dBi with an axial ratio of less than 1.1 dB is obtained. 4) Theoretical investigation of Gain Enhancement methods for the Yagi-like antennas printed in a multi-layer uniaxial anisotropic medium. It is shown that by a proper selection of anisotropy ratios and thickness of the layers, it is possible to obtain two high gain beams at θ_E and θ_H in E and H planes, respectively. In addition, the physics of these high gain fields are investigated in terms of the leaky-wave radiation.

14. SUBJECT TERMS
Printed Yagi-Like arrays, Multi-Layered Microstrip Antennas, Method of Moments, Gain Optimization, Evolutionary Programming

15. NUMBER OF PAGES
29

16. PRICE CODE

17. SECURITY CLASSIFICATION OF REPORT	18. SECURITY CLASSIFICATION OF THIS PAGE	19. SECURITY CLASSIFICATION OF ABSTRACT	20. LIMITATION OF ABSTRACT
UNCLASSIFIED	UNCLASSIFIED	UNCLASSIFIED	